Chemical Science

ROYAL SOCIETY OF CHEMISTRY

EDGE ARTICLE

View Article Online
View Journal | View Issue

Cite this: *Chem. Sci.*, 2024, **15**, 18067

All publication charges for this article have been paid for by the Royal Society of Chemistry

Received 21st July 2024
Accepted 16th September 2024

DOI: 10.1039/d4sc04843a

rsc.li/chemical-science

A homoleptic Ag^{III} complex stabilized by succinimidate ligands†

Emil Mickey Hilligsøe Larsen, [a] Theis Brock-Nannestad, [a] Jørgen Skibsted, [b] Anders Reinholdt *[ac] and Jesper Bendix *[a]

Herein, the first example of a homoleptic Ag^{III} complex stabilized by a monodentate N-donor ligand is presented. $Na_2[S_2O_8]$ oxidizes the linear Ag^{I} complex, $Na[Ag(succ)_2]$ ($\mathbf{1}^{Na}$), to form a square planar argentate(III) ion, $[Ag(succ)_4]^-$, which crystallizes with a polymeric chain-structure, $M[Ag(succ)_4]$ ($\mathbf{2}^{M}$), when treated with alkali metal sulfate M_2SO_4 (M = K, Rb, Cs). A mixed-valent Robin-Day class I system, $[(H_2O)Ag][Ag(succ)_4]$ ($\mathbf{2}^{Ag}$), forms in the absence of $K^+/Rb^+/Cs^+$ ion. Diamagnetic $\mathbf{2}^{Cs}$ displays a succinimide C=O stretching frequency at higher energy than does the isoelectronic Pd^{II} complex, $[(H_2O)Na]_2[Pd(succ)_4]$ ($\mathbf{3}^{Na}$). Moreover, $\mathbf{2}^{Cs}$ displays UV-vis absorptions that are more intense and occur at lower energy than those in $\mathbf{3}^{Na}$. The electron-deficient nature of $\mathbf{2}^{Cs}$ is further evident from its ability to oxidize water to O_2. From ^{109}Ag magic-angle spinning NMR studies, a highly deshielded Ag^{III} environment in $\mathbf{2}^{Cs}$ (2080 ppm) relative to the Ag^{I} starting material $\mathbf{1}^{Na}$ (492 ppm) is observed.

Introduction

Ag^{III} complexes remain elusive due to the limited selection of ligands that can coordinate to this high-valent metal center while resisting oxidation.[1] Accordingly, Ag^{III} complexes show utility as oxidizing agents,[2] and their electronic structure opens to applications in both superconducting[3] and semiconducting[4] materials. More recently, reductive elimination from the strongly oxidizing Ag^{III} ion has gained traction in $C(sp^3)$–$C(sp^3)$ coupling reactions[5] as well as cross-coupling of arenes, leading to heteroatom functionalization,[6] trifluoromethylation,[7] and alkylation.[8] The earliest examples of Ag^{III} complexes were bis(orthoperiodate)[9] and bis(orthotellurate)[10] complexes reported by Malaprade[9d] and by Malatesta[10], as well as an ethylenebis(biguanide) complex reported by Rây in 1943 (Chart 1A).[11] The stability of these classic Ag^{III} chelate complexes reflects both the ability of the ligands to resist oxidation as well as their ability to enforce square-planar coordination around the d^8 Ag^{III} ion. Along these lines, considerable development of Ag^{III} chemistry has revolved around chelating[12] and macrocyclic[13] ligands, in particular porphyrinoid systems[14] (Chart 1B). By contrast, homoleptic Ag^{III} systems with monodentate ligands, are confined to an exceedingly narrow range of oxidation-resistant donors: in 1957, Hoppe isolated the square planar fluoro complexes, $K[AgF_4]$ and $Cs[AgF_4]$,[15] (Chart 1C) and subsequently octahedral $Cs_2K[AgF_6]$ in 1966.[16] In 1968, Cohen and Atkinson generated $[Ag(OH)_4]^-$ in solution by anodic oxidation of silver;[17] this hydroxo complex could be trapped using periodate or tellurate as chelates (Chart 1A).[18] The reducing nature of nitrogen ligands has, heretofore, precluded

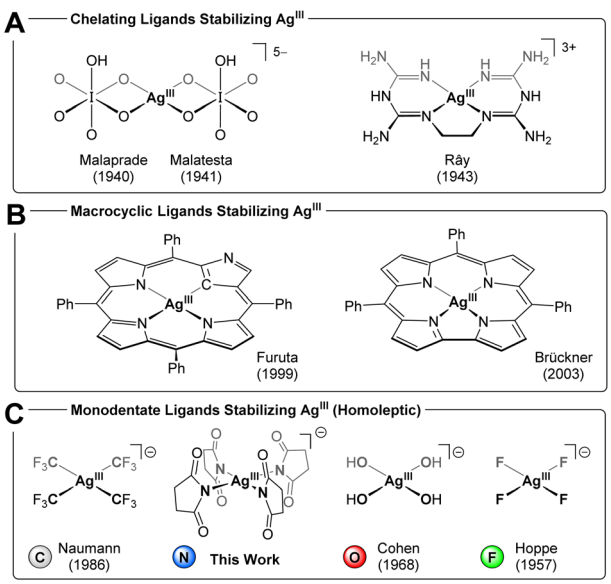

Chart 1 Ag^{III} complexes isolated using (A) chelating ligands, (B) macrocyclic ligands, (C) monodentate ligands.

[a]Department of Chemistry, University of Copenhagen, Universitetsparken 5, DK-2100 Copenhagen, Denmark. E-mail: bendix@kiku.dk

[b]Department of Chemistry and Interdisciplinary Nanoscience Center (iNANO), Aarhus University, Langelandsgade 140, DK-8000 Aarhus C, Denmark

[c]Department of Chemistry, Centre for Analysis and Synthesis, Lund University, P. O. Box 124, 22100 Lund, Sweden. E-mail: anders.reinholdt@chem.lu.se

† Electronic supplementary information (ESI) available: Synthetic procedures; NMR, IR, UV-vis, X-ray diffraction, and magnetic data. CCDC 2365916–2365920 and 2372376. For ESI and crystallographic data in CIF or other electronic format see DOI: https://doi.org/10.1039/d4sc04843a

unequivocal identification of any homoleptic Ag^{III} complex.[19] On the other hand, in 1986, Dukat and Naumann demonstrated how the $[Ag(CF_3)_2]^-$ ion disproportionates to metallic silver and the mixed-valent salt, $[Ag^{I}][Ag^{III}(CF_3)_4]$.[20] The remarkable stability of trifluoromethyl silver complexes[21] has since opened to isolation of numerous heteroleptic $[Ag(CF_3)_{4-n}(X)_n]^-$ argentate complexes (n = 1–3, X = halide, pseudohalide, hydrocarbyl)[7b,21a,22] as well as neutral $[Ag(CF_3)_3(L)]$ complexes (L = CH_3CN, PPh_3, $AsPh_3$, pyridine, *s*-2,4,6-trimethyltriazine, N-heterocyclic carbene).[23] More recently, Menjón and co-workers isolated a unique D_{3h}-symmetric $(Ph_4P)_2[Ag(CF_3)_2Br_3]$ complex,[24] ushering in five-coordinate geometries in Ag^{III} chemistry.[7,23b]

Akin to Ag^{III}, a square planar $(Ph_4P)[Cu(CF_3)_4]$ motif exists for the Cu^{III} ion.[25] Despite being d^8 Cu^{III} by customary electron counting rules,[26] this complex may be physically better described as a d^{10} Cu^{I} system bearing partially oxidized ligands, *i.e.* having an inverted ligand field (coined by Hoffmann).[27] This proposition was originally promulgated in a theoretical study by Snyder[28] and recently affirmed experimentally in X-ray spectroscopic studies by Lancaster[29] and high-resolution crystallographic studies by Overgaard.[30] Snyder extended the inverted ligand field description to square planar silver,[31] and against this background, it is interesting to consider electronic structure studies of Ag^{III} complexes. Grochala and Hoffmann studied binary and ternary silver fluorides by X-ray photoelectron spectroscopy and calculated density of states; for $K[AgF_4]$, the Ag 4d states contribute more to the ligand band than do the F 2p states.[32] In a similar fashion, Ghosh established how variously substituted [Ag(corrole)] complexes fall into both redox innocent, $[Ag^{[III]}(corrole^{[3-]})]$, and redox non-innocent, $[Ag^{[II]}(corrole^{[\cdot 2-]})]$, regimes.[14k,m] More recently, Menjón identified inverted ligand fields in a range of Ag^{III} complexes, including $[Ag(CF_3)_4]^-$, through experimental and computational studies.[22b,24] From an electronic structure standpoint, the d^8 Ag^{III} *versus* d^{10} Ag^{I} dichotomy represents two idealized points, $[Ag^{[+III]}(CF_3^{[-I]})_4]^-$ and $[Ag^{[+I]}(CF_3^{[-\frac{1}{2}]})_4]^-$, along a continuum of covalent interactions describing the Ag–CF_3 bond. The true electronic structure falls somewhere along this continuum, but, as the degree of covalency increases for higher oxidation states, the notion of electrons as belonging exclusively to any one metal- or ligand fragment inevitably breaks down. In a recent analysis of bonding in organometallic systems, Deeth pointed out that the oxidation state in $[Cu(CF_3)_4]^-$ reflects which bonding model is employed. While MO theory suggests an inverted LF with d^{10} Cu^{I}, the *ai*LFT subspace modeling implemented in the ORCA program package suggests a normal LF with a square planar d^8 Cu^{III}, leading to the salient conclusion that these are very covalent systems no matter the modeling approach.[33] Inspired by the elusive nature and enticing electronic structure of Ag^{III} complexes, we sought strongly donating ligands to stabilize the high oxidation state. Considering Collins's seminal work on high-valent amide complexes (including Cu^{III}),[34] coupled with the ability of halosuccinimides to act as synthons for oxidized species such as Cl^+ and Br^+, we inquired whether the succinimide anion ($succ^-$) could stabilize a homoleptic Ag^{III} complex. Herein, we present the synthesis of a square-planar argentate(III) ion, $[Ag(succ)_4]^-$, isolated as polymeric Cs^+, Rb^+, and K^+ salts. We also present the isolation of a mixed-valent $[(H_2O)Ag^{I}][Ag^{III}(succ)_4]$ salt. We probe the electronic structure of the highly oxidized Ag^{III} complex alongside the isoelectronic Pd^{II} analog, $[Pd(succ)_4]^{2-}$, combining vibrational, UV-visible, and solid-state ^{109}Ag NMR spectral data.

Results and discussion

Synthesis of a succinimide-stabilized Ag^{III} complex (2^{Cs})

Succinimide buffers have emerged as non-toxic alternatives to cyanide baths for electrodeposition of silver,[35] and accordingly, Ag^{I}/$succ^-$ systems have been subject to a wide range of electrochemical studies. In one study, Lessard observed that $[M][Ag(succ)_2]$ complexes (M^+ = Ag^+, Et_4N^+) undergo an oxidation process in acetonitrile, whose limiting current increases when excess succinimide anion is present.[36] In a subsequent study, the oxidation product was proposed to be succinimidyl radical, succ$^\cdot$, based on the isolation of free succinimide formed upon H-atom abstraction from the solvent.[37] In a separate study, Masaki reported that silver anodes develop a crystalline covering in aqueous succinimide buffers, assigned to a rare Ag^{II} species, such as $[Ag(succ)_2]$.[38] Given that $Na_2[S_2O_8]$ oxidizes $AgNO_3$ in pyridine to afford the orange and paramagnetic Ag^{II} complex, $[Ag(pyridine)_4][S_2O_8]$,[39] we conducted a chemical oxidation of $AgNO_3$ in aqueous succinimide buffer, using $Na_2[S_2O_8]$. Heating the solution converted the *in situ* generated Ag^{I} complex, Na $[Ag(succ)_2]$ ($\mathbf{1^{Na}}$), to a new yellow-colored species, which could be isolated in good yield as large, bright yellow crystals by addition of Cs_2SO_4 (54%) or Rb_2SO_4 (45%), and low yield (11%) from solutions containing only K(succ) (Scheme 1). The new species could also be prepared by electrocrystallization. In a two-chamber system with a silver cathode in aqueous $AgNO_3$ and a platinum anode in a succinimide buffer containing Cs_2SO_4 and $AgNO_3$, the new species deposits on the anode when the potential difference exceeds 0.80 V. The surface area of the anode limits the yield from electrocrystallization ($\sim$1 mg cm^{-2}), and thus, chemical oxidation is most suitable for generating larger quantities of the new species.

The color of the new species isolated in our studies (yellow) differs strikingly from Masaki's putative $[Ag(succ)_2]$ complex (white), which called for further characterization. Interestingly, ^1H and ^{13}C NMR spectra of solutions (D_2O) of the new species showed sharp singlets in the normal chemical shift range for succinimide complexes, and solid-state DC SQUID magnetometry studies ($\chi_M = -1.2 \times 10^{-4}$ cm^3 mol^{-1}, 70–300 K) affirmed a diamagnetic system, which would be inconsistent with a magnetically uncoupled Ag^{II} complex. Electrospray ionization mass spectrometry (ESI-MS) in negative mode revealed a molecular ion with m/z corresponding to $[Ag(succ)_4]^-$, as well as heavier aggregates, $\{Cs[Ag(succ)_4]_2\}^-$ and $\{Cs_2[Ag(succ)_4]_3\}^-$. In line with the other characterization data, X-ray crystallographic studies revealed the new species to be a salt of composition $Cs[Ag(succ)_4]\cdot 4H_2O$ ($\mathbf{2^{Cs}}$, spacegroup $I4/m$, Fig. 1A). The silver ion resides at the intersection between a mirror-plane and a fourfold axis, with the nitrogen-bound succinimide ligands oriented perpendicular to the square planar silver ion. The carbonyl oxygens from two $[Ag(succ)_4]^-$

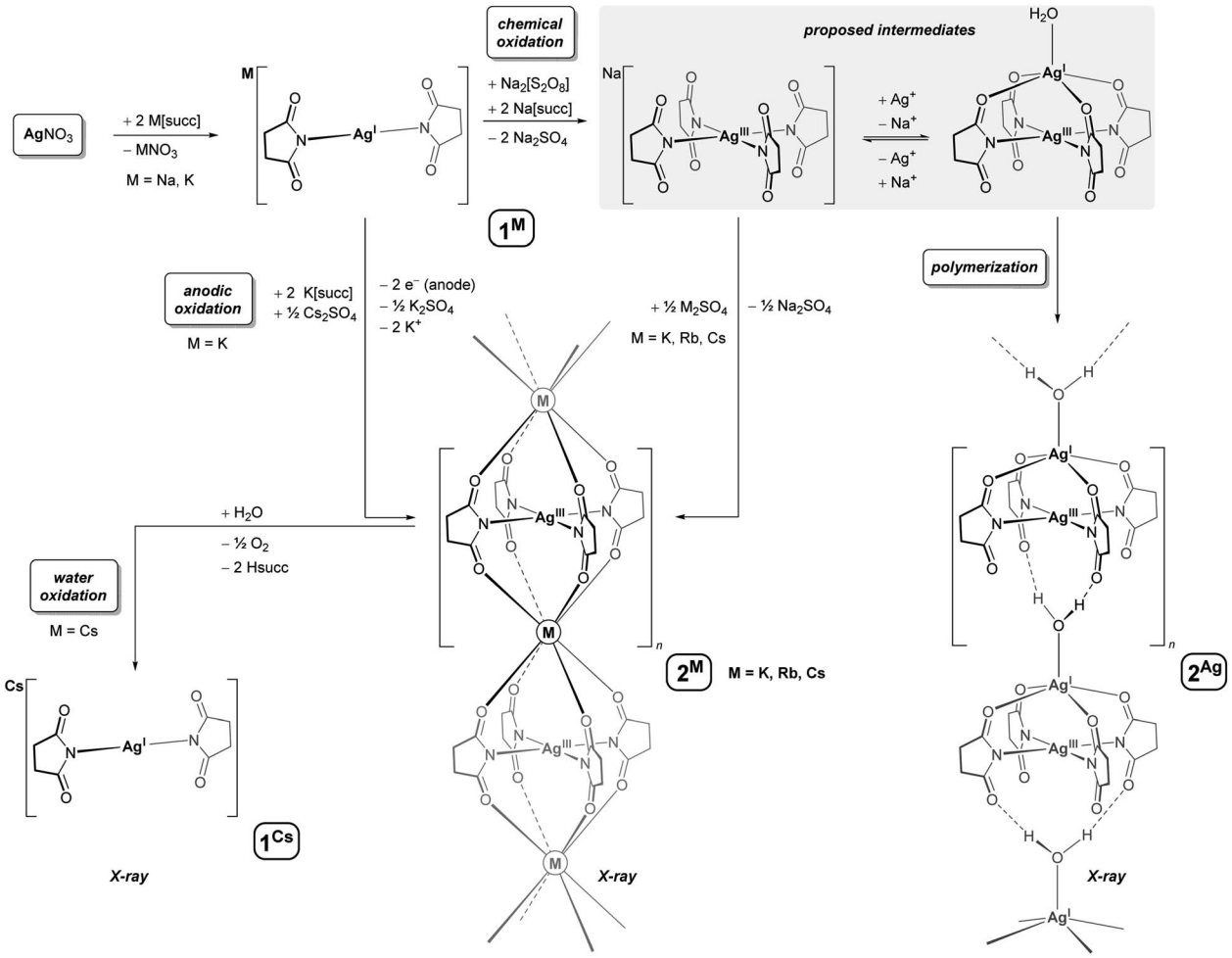

Scheme 1 Chemical or anodic oxidation converts $[Ag(succ)_2]^-$ to a square-planar argentate(III) ion, $[Ag(succ)_4]^-$; complexation with Cs^+, Rb^+, K^+, or Ag^+ yields polymeric salts, 2^{Cs}, 2^{Rb}, 2^{K}, and 2^{Ag}. Complex 2^{Cs} oxidizes water to form 1^{Cs} and O_2.

ions coordinate to the cesium ion, generating an elongated square prismatic motif (O···O edges: 2 × 3.275(3), 1 × 4.206(2) Å), while four molecules of water engage in hydrogen bonding with the same carbonyl oxygens, resulting in a polymeric chain-structure (Fig. 1B). Bond distances in the isostructural rubidium derivative, $Rb[Ag(succ)_4]\cdot 4H_2O$ (2^{Rb}), reflect the smaller ionic radius of Rb^+ *versus* Cs^+ (O···O edges: 2 × 3.253(2), 1 × 3.967(2) Å), whereas metrics within the $[Ag(succ)_4]^-$ ion are essentially unperturbed. A similar situation is observed for the potassium derivative, $K[Ag(succ)_4]\cdot 4H_2O$ (2^{K}), given the even smaller ionic radius for K^+ (O···O edges: 2 × 3.242(2), 1 × 3.880(2) Å). The Ag–N bonds in 2^{Cs} (2.009(3) Å) are short compared to the range known for $[Ag^{I}(succ)_2]^-$ complexes (2.067(5)–2.088(2) Å),[40] and in fact, the Ag–N bond distance in 2^{Cs} falls among the shortest 0.5% Ag–N bond distances in the Cambridge Structural Database, in line with the presence of a contracted Ag^{III} ion in 2^{Cs}.

DFT computational assignment of the silver oxidation state in 2^{Rb}

The assignment of a high formal oxidation state of +III for silver bound to mono-anionic succinimidate ligands appears reasonable based on the structural data. However, for high-valent, late transition metals, the question of ligand non-innocence leading to internal redox and concomitant inverted ligand fields has received increasing focus as described above.[22b,24,27–33] In order to gauge the level of covalency and the appropriateness of the Ag^{III} formulation, we performed a single point DFT calculation employing the B3LYP functional and the experimental geometry for 2^{Rb} with two Rb^+ cations terminating the silver complex and yielding a mono cationic fragment for the computation. As the DFT is known to be biased towards covalent description of the M–L bonding,[41] the results are expected to represent an upper estimate on the covalency. The system is very covalent as indicated by a low Mulliken charge on the Ag (+0.22) and only a fractional hole (0.77 e) in the silver d-shell. The σ-interaction between Ag and the succinimidate ligands has an anti-bonding part, which in the normal LF ordering should be a pure, unoccupied $4d_{x^2-y^2}$(Ag) orbital. The KS-LUMO is indeed the one with most $4d_{x^2-y^2}$(Ag) character among all of the orbitals, but the Ag-$d_{x^2-y^2}$ contribution totals only 35%. A plot of the LUMO is given in Fig. S35† illustrating the delocalization throughout the complex. The bonding counterpart has only *ca.* 12% of Ag-$d_{x^2-y^2}$ contribution

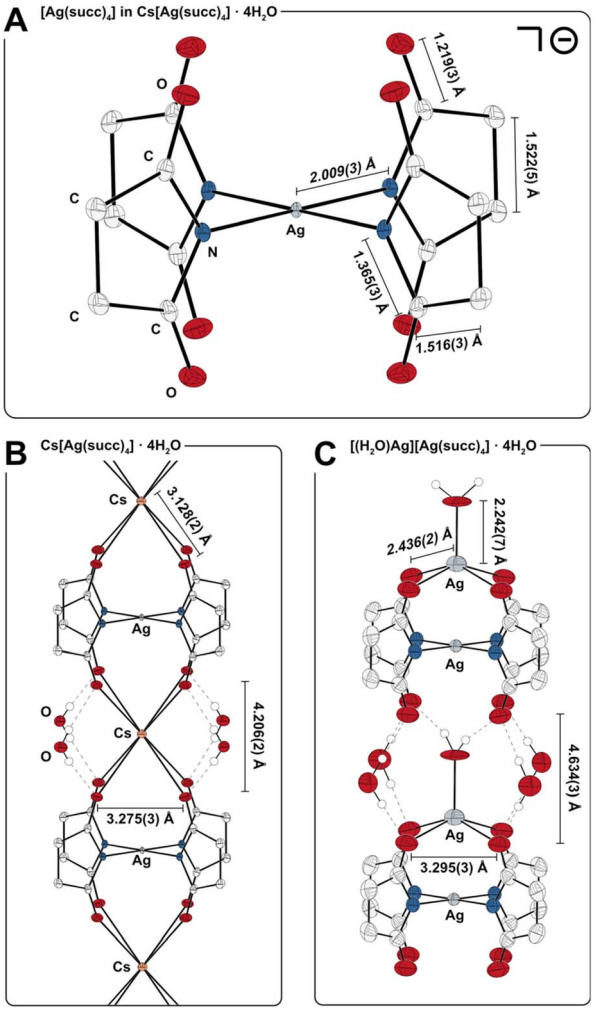

Fig. 1 X-ray crystallographic studies (H atoms omitted, except on H_2O). (A) Geometry of the $[Ag(succ)_4]^-$ ion in $\mathbf{2^{Cs}}$ (50% probability, 122(2) K). (B) Bonding interactions between C=O groups, Cs^+, and H_2O in the polymeric chain-structure of $\mathbf{2^{Cs}}$. (C) Bonding interactions between C=O groups, Ag^+, and H_2O in the polymeric structure of $\mathbf{2^{Ag}}$ (30% probability, 293(2) K); orientational disorder of the $[H_2O–Ag]^+$ unit is omitted.

(Fig. S35,† bottom), which aligns with a non-inverted LF, but the remaining *ca.* 45% of Ag-$d_{x^2-y^2}$ is shared between many, mainly bonding, KS-orbitals. In summary, the DFT data suggest that the complex is borderline between having a normal and an inverted ligand field. Considering the covalency bias of the DFT calculations on transition metal complexes, we employ the classical LF picture with an empty $4d_{x^2-y^2}$(Ag) orbital for the remaining discussions. Similar modeling of the Ag^I salt of $[Ag(succ)_4]^-$ (*vide infra*) yielded a clear distinction between the two silver centers with the Ag^{III} having the lower Mulliken charge (+0.11 *versus* +0.49 for Ag^I), but with Mayer total valencies of 2.52 *versus* 0.98 for the high and low valent Ag-centers.

Isolation of a mixed-valent Ag^I–Ag^{III} complex ($\mathbf{2^{Ag}}$)

Complex $\mathbf{2^{Cs}}$ was reproducibly isolated in 50–55% yield when $AgNO_3$ was used as the limiting reagent, and modification of the synthetic procedure did not increase the yield. When left to crystallize, yellow reaction mixtures containing $[Ag(succ)_4]^-$ and Cs_2SO_4 produce very little crystalline material over an initial period of two days, whereas the solutions typically decolorize and deposit large amounts of yellow crystals of $\mathbf{2^{Cs}}$ after three days. Addition of a solution of NaCl to the isolated mother liquor resulted in precipitation of AgCl within seconds, demonstrating the presence of an unreacted Ag^I species, after crystallization of $\mathbf{2^{Cs}}$ is complete. In view of these observations, we further examined reaction mixtures containing the $[Ag(succ)_4]^-$ ion. By heating a concentrated solution containing Na(succ), $AgNO_3$, and $Na_2[S_2O_8]$ in a molar ratio of 4 : 2 : 1, we isolated dark yellow crystals within few minutes. The resulting tetragonal crystalline phase has crystallographic *a*- and *b*-axes similar to $\mathbf{2^{Cs}}$/$\mathbf{2^{Rb}}$/$\mathbf{2^{K}}$, but a longer *c*-axis, indicative of a $[Ag(succ)_4]^-$ system with a larger spacer between the Ag^{III} centers. Solving the crystal structure revealed a polymeric, mixed-valent salt of composition $[(H_2O)Ag][Ag(succ)_4]\cdot 4H_2O$ ($\mathbf{2^{Ag}}$, spacegroup *I*4/*m*, Fig. 1C). The $[(H_2O)Ag]^+$ fragment is located between four of the carbonyl oxygens from a $[Ag(succ)_4]^-$ unit, forming a square pyramidal motif with water at the apical position (τ_5 = 0.00).[42] The apical water molecule forms hydrogen bonds to the free set of carbonyl oxygens from a neighboring $[(H_2O)Ag][Ag(succ)_4]$ fragment, generating a polymeric structure. Given that the $[Ag(succ)_4]^-$ fragment resides at the intersection between a crystallographic four-fold rotation axis and a mirror plane, the $[(H_2O)Ag]^+$ fragments are disordered over two orientations, pointing in either direction of the polymeric chain structure. The $[(H_2O)Ag]^+$ fragments separate neighboring $[Ag(succ)_4]^-$ units in $\mathbf{2^{Ag}}$ more effectively than Cs^+, Rb^+, and K^+ do in $\mathbf{2^{Cs}}$/$\mathbf{2^{Rb}}$/$\mathbf{2^{K}}$, resulting in a significantly elongated square prismatic motif in $\mathbf{2^{Ag}}$ (O···O edges: 2 × 3.295(3), 1 × 4.634(3) Å). Overall, $\mathbf{2^{Ag}}$ conforms to a Robin-Day class I description,[43] given its structure and spectroscopic traits: The $[Ag(succ)_4]^-$ fragments in $\mathbf{2^{Cs}}$, $\mathbf{2^{Rb}}$, $\mathbf{2^{K}}$, and $\mathbf{2^{Ag}}$ display the same gross geometry. On the other hand, a structurally distinct $[(H_2O)Ag]^+$ site is present in $\mathbf{2^{Ag}}$, suggesting distinctly different oxidation states in the mixed-valent salt. Moreover, the UV-vis spectrum of $\mathbf{2^{Ag}}$ is devoid of intervalence charge-transfer bands and is essentially superimposable with that of $\mathbf{2^{Cs}}$ (see discussion below as well as ESI, Fig. S12†). Returning to the observation that isolated yields of $\mathbf{2^{Cs}}$ are consistently close to 50%, we propose that a monomeric species akin to $\mathbf{2^{Ag}}$ forms in equilibrium in the reaction mixtures. The Ag^+ ion would prevent Cs^+ from coordinating to the argentate(III) ion, $[Ag(succ)_4]^-$, to form polymeric $\mathbf{2^{Cs}}$. Once the substitution of Ag^+ for Cs^+ eventually succeeds, most of the oxidant, $Na_2[S_2O_8]$ may have then been consumed in other oxidation processes, leaving close to half of the Ag^I ions untouched.

Isolation of a Pd^{II} complex ($\mathbf{3^{Na}}$) and comparison to the isoelectronic Ag^{III} complex ($\mathbf{2^{Cs}}$)

To assess how the trivalent silver ion affects the molecular and electronic structure of the $[Ag(succ)_4]^-$ anion, we prepared the isoelectronic palladium anion, $[Pd(succ)_4]^{2-}$, by dissolving

$[PdCl_2]$ in succinimide buffer. From the reaction mixture, colorless crystals of $[(H_2O)Na]_2[Pd(succ)_4]\cdot 2H_2O$ ($\mathbf{3^{Na}}$) were isolated in 77% yield and characterized by elemental analysis, ^1H and ^{13}C NMR spectroscopies, ESI-MS, and X-ray crystallography (Chart 2A). The $[Pd(succ)_4]^{2-}$ fragment adopts a gross geometry akin to the Ag^{III} analog, with Pd–N bond distances that are statistically indistinguishable from Ag–N bond distances in $\mathbf{2^{Cs}}$ (Chart 2B). Given the larger ionic radius of Pd^{II} as compared to the more contracted Ag^{III} ion, these metrics indicate that metal-succinimide bonding in $\mathbf{2^{Cs}}$ and $\mathbf{3^{Na}}$ might display variable degrees of covalency. In complex $\mathbf{3^{Na}}$, the two sets of carbonyl oxygens from the $[Pd(succ)_4]^{2-}$ ion coordinate to one Na^+ ion above – and one below – the plane of the Pd^{II} center, and the coordination sphere of each Na^+ ion is completed by an axial water molecule to form a square pyramidal motif ($\tau_5 = 0.02$). In complex $\mathbf{3^{Na}}$, the relatively small Na^+ ion adopts a buried position between the four carbonyl oxygens, similar to the Ag^+ ion in $\mathbf{2^{Ag}}$ ($\mathbf{3^{Na}}$: $Pd^{II}\cdots Na = 3.0321(5)$ Å, $\mathbf{2^{Ag}}$: $Ag^{III}\cdots Ag^{I} = 2.972(1)$ Å). In contrast, the Cs^+, Rb^+, and K^+ ions in $\mathbf{2^{Cs}}$, $\mathbf{2^{Rb}}$, and $\mathbf{2^{K}}$ show a more pronounced departure from the Ag^{III} centers ($Ag^{III}\cdots Cs = 4.3722(2)$ Å, $Ag^{III}\cdots Rb = 4.2535(3)$ Å, $Ag^{III}\cdots K = 4.2066(2)$ Å). This highlights the role of the counterion, as well as hydrogen bonding interactions, in the isolation of the polymeric Ag^{III} salts, $\mathbf{2^{Cs}}$, $\mathbf{2^{Rb}}$, $\mathbf{2^{K}}$, and $\mathbf{2^{Ag}}$.

We then turned to spectroscopic methods to glean more information about the electronic structure of the Ag^{III}, Pd^{II}, and Ag^{I} systems, $\mathbf{2^{Cs}}$, $\mathbf{3^{Na}}$, and $\mathbf{1^{Na}}$ (Chart 2B). The IR spectrum of crystalline $\mathbf{2^{Cs}}$ is dominated by a strong out-of-phase[44] C=O stretching frequency at 1654 cm^{-1} (this is also the case for $\mathbf{2^{Rb}}$ and $\mathbf{2^{K}}$). In contrast, Pd^{II} complex $\mathbf{3^{Na}}$ displays a C=O vibration at 1630 cm^{-1}, and Ag^{I} precursor $\mathbf{1^{Na}}$ displays a C=O vibration at 1615 cm^{-1}. In this series ($Ag^{III} > Pd^{II} > Ag^{I}$), the shift of the C=O vibrations toward lower frequencies illustrates how the succinimide anion is sensitive to the oxidation state of the metals. This reflects a balance between the succinimide ligand, on the one hand, being engaged in donor interactions to stabilize a high-valent metal ion such as Ag^{III}, or, on the other hand, forming a delocalized π-system involving the carbonyl and imide nitrogen groups. Accordingly, C=O bond distances in complex $\mathbf{3^{Na}}$ are elongated by ~0.01 Å (avg. 1.232(2) Å) as compared to complex $\mathbf{2^{Cs}}$. From NMR measurements, the ^1H resonance of $\mathbf{2^{Cs}}$ in D_2O displays a singlet at 2.78 ppm, whereas $\mathbf{3^{Na}}$ displays a more shielded proton environment (2.50 ppm), in accord with the lower negative charge and higher oxidation state of the $[Ag(succ)_4]^-$ anion *versus* $[Pd(succ)_4]^{2-}$. By contrast, the carbonyl ^{13}C NMR resonance in $\mathbf{2^{Cs}}$ is *more* shielded than that in $\mathbf{3^{Na}}$, in line with the shorter C=O bond in the Ag^{III} complex leading to a more efficient orbital overlap within the carbonyl group, and hence a more shielded carbon nucleus.

UV-visible spectroscopic studies of a Ag^{III} complex ($\mathbf{2^{Cs}}$)

Given the bright yellow color of complex $\mathbf{2^{Cs}}$, we subjected an aqueous sample to UV-visible spectroscopy (Fig. 2). The Ag^{III} complex displays a very strong UV absorption at 222 nm ($\varepsilon = 19\,400\ M^{-1}\ cm^{-1}$), with energy and intensity falling close to 4 eq. of free succinimidate (215 nm, $\varepsilon = 5900\ M^{-1}\ cm^{-1}$, see ESI Fig. S15†). Moreover, $\mathbf{2^{Cs}}$ displays two intense bands in the near-UV range at 302 and 361 nm (ε = 8100, 4300 $M^{-1}\ cm^{-1}$, Fig. 2A); the lowest-energy band extends into the visible range and vanishes around 500 nm, accounting for the yellow color of the complex. In a similar fashion, aqueous solutions of $\mathbf{2^{Ag}}$ display absorptions at energies essentially identical to those of $\mathbf{2^{Cs}}$ but with ~50% higher intensity, in line with the darker yellow color of the mixed-valent silver complex.

Comparison of $\mathbf{2^{Cs}}$ and $\mathbf{2^{Ag}}$ in the solid state (KBr pellet) reveals very similar UV-vis features, in accord with the solution data (ESI, Fig. S12 and S13†). We also recorded UV-visible spectral data for the isoelectronic $[Pd(succ)_4]^{2-}$ anion in $\mathbf{3^{Na}}$. Akin to $\mathbf{2^{Cs}}$, the palladium complex exhibits a very strong UV-absorption at 216 nm ($\varepsilon = 49\,100\ M^{-1}\ cm^{-1}$) as well as two bands in the near-UV range (289, 336 nm, ε = 290, 120 $M^{-1}\ cm^{-1}$), which exhibit a similar band shape to $\mathbf{2^{Cs}}$. However, Pd^{II} complex $\mathbf{3^{Na}}$ displays markedly lower absorption intensity than the trivalent silver system $\mathbf{2^{Cs}}$ (×1/30, Fig. 2A, inset). The qualitatively similar appearance of electronic transitions observed for $[Ag(succ)_4]^-$ and $[Pd(succ)_4]^{2-}$ is indicative of these isoelectronic complexes possessing similar electronic structures. In view of the more oxidizing nature of the Ag^{III} ion as compared to Pd^{II}, complex $\mathbf{2^{Cs}}$ displays electronic transitions with more ligand-to-metal charge-transfer character, resulting in lower transition energies and higher molar absorptivity. TDDFT calculation on $\mathbf{2^{Rb}}$ yielded three states with significant intensities with wavelengths of 372, 346 and 247 nm, of which the two lowest energy transitions involved excitations from

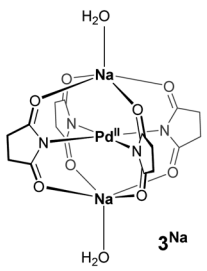

Complex		$\mathbf{2^{Cs}}$	$\mathbf{3^{Na}}$	$\mathbf{1^{Na}}$
Oxidation State		+III	+II	+I
$\tilde{\nu}_{C=O}$	(cm^{-1})	1654	1630	1615
δ_H	(ppm)	2.78	2.50	
$\delta_{C=O}$	(ppm)	187.4	194.2	
$d_{C=O}$	(Å)	1.219(3)	1.227(2) 1.231(2) 1.234(2) 1.238(2)	1.23(2)^{avg}
d_{Ag-M}	(Å)	2.009(3)	2.004(1) 2.011(1)	2.07(1)^{avg}

Chart 2 (A) Molecular structure of $\mathbf{3^{Na}}$. (B) Spectroscopic and metric data for succinimide complexes $\mathbf{2^{Cs}}$ (Ag^{III}), $\mathbf{3^{Na}}$ (Pd^{II}), and $\mathbf{1^{Na}}$ (Ag^{I}).

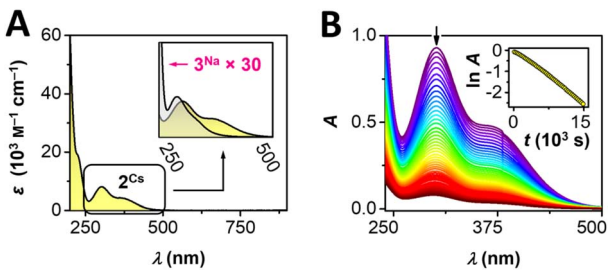

Fig. 2 (A) UV-vis spectroscopic studies of $\mathbf{2^{Cs}}$ and $\mathbf{3^{Na}}$. (B) Evolution of UV-vis spectra of $\mathbf{2^{Cs}}$ in neutral solution; inset: time dependence of ln*A* at λ_{max} = 302 nm.

bonding orbitals of mainly ligand character to the heavily admixed LUMO having the most $4d_{x^2-y^2}$ (Ag) character of any of the KS-orbitals. The transition at 346 nm is calculated as the most intense by a factor of 10. The change in electron density for this transition shows a shift of electron density from the succ-$\pi^{\perp}$ orbitals involving the nitrogen and carbonyl groups towards the σ-orbitals on silver and nitrogen (*cf.* Fig. S36†). This corroborates the description of the transitions as having significant LMCT character. The high-valent nature of $\mathbf{2}^{\mathbf{Cs}}$ can be further ascertained from its ability to oxidize water (Scheme 1). In aqueous solution, electronic transitions between 250–500 nm decrease in a first-order process with a half-life of 70 minutes (293 K, Fig. 2B). The process proceeds with formation of O_2, succinimide, and a new Ag^{I} complex, $Cs[Ag(succ)_2]\cdot 4H_2O$ ($\mathbf{1}^{\mathbf{Cs}}$), identified by a combination of NMR spectroscopy and X-ray crystallography. These findings are interesting given Lessard's suggestion that electrochemical oxidation of $[Ag(succ)_2]^-$ affords a succinimidyl radical, which acts as a hydrogen atom abstractor to form succinimide;[37] our studies, on the other hand, implicate a Ag^{III} complex.

Solid-state ^{109}Ag NMR spectroscopic studies of a Ag^{III} complex ($\mathbf{2}^{\mathbf{Cs}}$)

Given the tendency for $\mathbf{2}^{\mathbf{Cs}}$ to decay in aqueous solution, clean NMR spectral data can be recorded within a timeframe of ~5 minutes after a sample of $\mathbf{2}^{\mathbf{Cs}}$ has been prepared. This permits characterization of reasonably sensitive nuclei, such as ^{1}H and ^{13}C. In view of the lower sensitivity of a nucleus such as ^{109}Ag, we conducted a solid-state NMR spectroscopic study of $\mathbf{2}^{\mathbf{Cs}}$ to gain more information about the trivalent silver ion. ^{109}Ag magic-angle spinning (MAS) NMR spectra (14.09 T) were recorded for monovalent complex $\mathbf{1}^{\mathbf{Na}}$ and trivalent complex $\mathbf{2}^{\mathbf{Cs}}$ (Fig. 3). The acquisition of these solid-state NMR spectra is complicated by the low gyromagnetic ratio for ^{109}Ag, as well as long spin-lattice relaxation times (T_1's), which may be on the order of several hundred seconds for diamagnetic silver compounds.[45] Accordingly, single-pulse ^{109}Ag NMR spectra were recorded with relaxation delays of 180–600 s (not corresponding to full relaxation), resulting in rather low signal-to-noise ratios even at acquisition times spanning several days. Both of the complexes, $\mathbf{1}^{\mathbf{Na}}$ and $\mathbf{2}^{\mathbf{Cs}}$, displays a single isotropic peak, which in each case is flanked by one or two rotational spinning sidebands on each side, due to ^{109}Ag chemical shift anisotropy (CSA). The intensities of the centerband and spinning sidebands allow estimation of the ^{109}Ag CSA parameters from spectral simulations for $\mathbf{1}^{\mathbf{Na}}$ and $\mathbf{2}^{\mathbf{Cs}}$ (Table 1).

A clear distinction in isotropic chemical shifts is apparent for the two complexes, with $\mathbf{1}^{\mathbf{Na}}$ displaying an isotropic shift at 492 ppm, whereas trivalent $\mathbf{2}^{\mathbf{Cs}}$ gives rise to a much more deshielded isotropic shift at 2080 ppm at the same spinning frequency and sample temperature. In this regard, $\mathbf{1}^{\mathbf{Na}}$ and $\mathbf{2}^{\mathbf{Cs}}$ show a similar correlation between oxidation state and chemical shift as observed between a Ag^{I} complex such as $[Ag(CF_3)_2]^-$ (566 ppm) and a covalent Ag^{III} complex such as $[Ag(CF_3)_4]^-$ (2233 ppm).[22a] Generally speaking, monovalent Ag^{I} compounds, including oxides[45b–d,48] and nitrogen-coordinated complexes,[45a,49] exhibit ^{109}Ag chemical shifts in the range −100 to +1000 ppm. Trivalent silver complexes, on the other hand, display strongly deshielded resonances, often in the

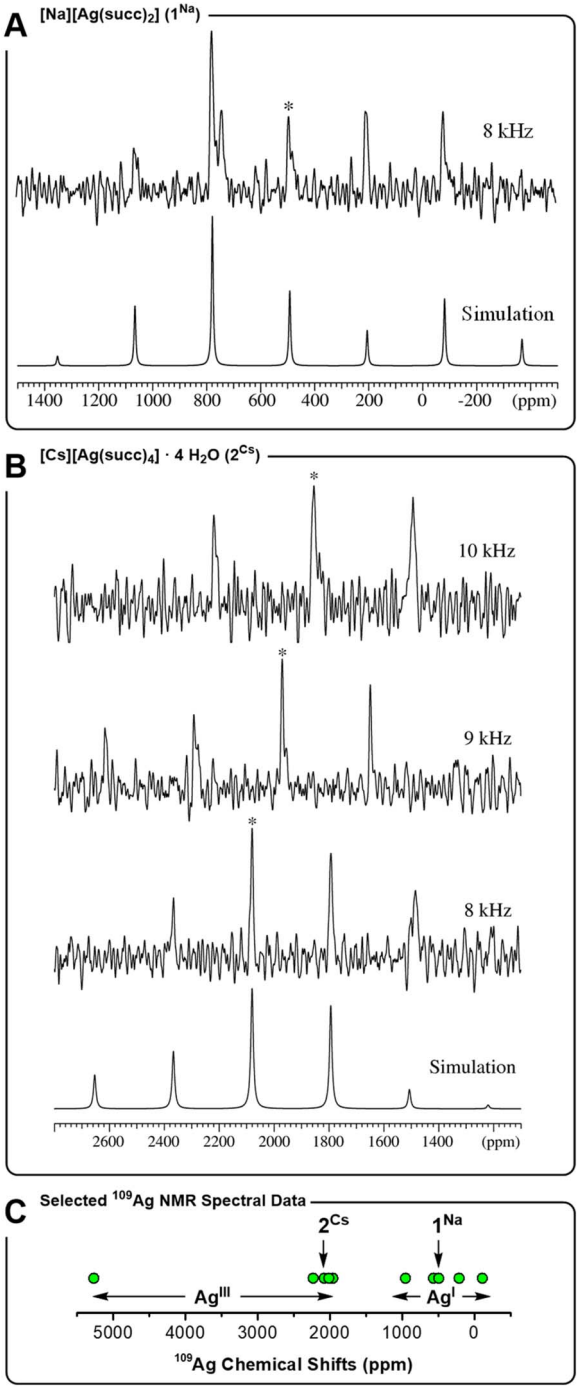

Fig. 3 ^{109}Ag MAS NMR spectra 14.09 T (27.9 MHz). (A) $\mathbf{1}^{\mathbf{Na}}$ measured at a spinning frequency of $\upsilon_R = 8.0$ kHz ($T = 36$ °C, relaxation delay $d1 = 180$ s, 2304 scans). (B) $\mathbf{2}^{\mathbf{Cs}}$ measured at spinning frequencies of $\upsilon_R = 10.0$ kHz ($T = 43$ °C, $d1 = 600$ s, 542 scans), 9.0 kHz ($T = 40$ °C, $d1 = 300$ s, and 1356 scans) and 8.0 kHz ($T = 36$ °C, $d1 = 600$ s, and 1004 scans). Isotropic peaks indicated by *. (C) Representative ^{109}Ag chemical shifts (ppm) for Ag^{III} and Ag^{I} complexes: $[Ag^{III}F_4]^-$ (5270),[46] $[Ag^{III}(CF_3)_4]^-$ (2233),[22a] $\mathbf{2}^{\mathbf{Cs}}$ (2080), $Ag^{III}{}_2O_3$ (2015),[45b] $Ag^{I}Ag^{III}O_2$ (1960),[45b] $Ag^{I}AlO_2$ (953),[45b] $[Ag^{I}(CF_3)_2]^-$ (566),[22a,47] $\mathbf{1}^{\mathbf{Na}}$ (492), $[Ag^{I}N(SO_2Me)_2]$ (210),[45d] $Ag^{I}F$ (−110).[45d]

Table 1 ^{109}Ag chemical shift parameters for $\mathbf{1}^{Na}$ and $\mathbf{2}^{Cs}$

	υ_R (kHz)	T (°C)	δ_{iso}[a] (ppm)	δ_σ[b] (ppm)	η_σ[b]
$\mathbf{1}^{Na}$	8.0	36	492 ± 2	1100 ± 100	0.2 ± 0.2
$\mathbf{2}^{Cs}$	8.0	36	2080 ± 2	−750 ± 100	0.5 ± 0.2
	9.0	40	1971 ± 2	n.d.	n.d.
	10.0	43	1855 ± 2	n.d.	n.d.

[a] ^{109}Ag isotropic chemical shift referenced to a 1.0 M $AgNO_3$ solution (T = 21 °C). At these conditions, $\delta_{iso} = -118 \pm 1$ ppm is observed for solid $AgNO_3$ at T = 43 °C. [b] ^{109}Ag chemical shift anisotropy parameters, defined as $\delta_{iso} = \frac{1}{3}(\delta_{xx} + \delta_{yy} + \delta_{zz})$, $\delta_\sigma = (\delta_{iso} - \delta_{zz})$, and $\eta_\sigma = (\delta_{xx} - \delta_{yy})/\delta_{zz}$, where δ_{xx}, δ_{yy}, and δ_{zz} are the principal elements of the chemical shift tensor defined as $|\delta_{zz} - \delta_{iso}| \geq |\delta_{xx} - \delta_{iso}| \geq |\delta_{yy} - \delta_{iso}|$.

range 1900 to 2500 ppm, and even as high as 5270 ppm for $K[AgF_4]$ (Fig. 3C). Thereby, the ^{109}Ag MAS NMR spectra support the presence of a Ag^{III} center in complex $\mathbf{2}^{Cs}$, and the observation of a unique Ag^{III} site by NMR is in accord with the crystallographic symmetry. Furthermore, ^{109}Ag CSA parameters (δ_σ and η_σ) were determined, albeit with rather low precision, reflecting the low S/N ratio of the acquired spectra. Notably, the shielding anisotropy (δ_σ) changes sign between $\mathbf{1}^{Na}$ and $\mathbf{2}^{Cs}$. This is in line with the change in geometry about the silver ion, going from axial donation in linear $\mathbf{1}^{Na}$ to equatorial donation in square planar $\mathbf{2}^{Cs}$. Finally, we note that $\delta_{iso}(^{109}Ag)$ is highly temperature dependent for $\mathbf{2}^{Cs}$, as apparent from the spectra obtained at different spinning frequencies, causing different degrees of frictional heating of the sample. The chemical shifts observed at three different rotation frequencies (Table 1), indicate δ_{iso} to have a temperature dependence of −32 ppm/°C, leading to a variation of several hundred ppm within a few °C (in contrast, $\mathbf{1}^{Na}$ displays no temperature dependence of δ_{iso} over the small studied temperature range of ±5 °C). Although not record-setting, the temperature dependence of the chemical shift for $\mathbf{2}^{Cs}$ is quite large for a d-block metal.[50] Moreover, it is clear that comparisons of the numerical value of ^{109}Ag NMR chemical shifts for Ag^{III} complexes (such as those in Fig. 3C), should be made with care, given the effect of temperature.

Conclusions

In summary, we have isolated the first example of a homoleptic and square planar Ag^{III} complex stabilized by a monodentate N-donor ligand, namely the Cs^+, Rb^+, K^+, and Ag^+ salts of the argentate(III) ion $[Ag(succ)_4]^-$ ($\mathbf{2}^{Cs}$, $\mathbf{2}^{Rb}$, $\mathbf{2}^{K}$, and $\mathbf{2}^{Ag}$). Dissolving $AgNO_3$ in succinimide buffer affords Ag^I precursor $\mathbf{1}^{Na}$, which is oxidized chemically by $Na_2[S_2O_8]$ or electrochemically by anodic oxidation to form a square planar $[Ag(succ)_4]^-$ motif. Complexation with Cs^+, Rb^+, K^+, or Ag^+ leads to polymeric chain-structures, which in the case of $\mathbf{2}^{Ag}$ encompasses a mixed-valent Robin-Day class I system. ^{1}H and ^{13}C NMR spectral studies combined with SQUID magnetometry attest to the diamagnetic nature of $\mathbf{2}^{Cs}$. IR spectroscopy reveals a high-frequency C=O stretching mode for the succinimide ligands in $\mathbf{2}^{Cs}$ as compared to the isoelectronic Pd^{II} complex, $\mathbf{3}^{Na}$. DFT modeling of the ground state electronic structure suggests the systems to be placed at the border between having a normal LF (Ag^{III}) and an inverted LF (Ag^I). In addition, UV-vis spectroscopy reveals electronic transitions at lower energy and with higher molar absorption for $\mathbf{2}^{Cs}$ than for $\mathbf{3}^{Na}$. These spectroscopic results point to the oxidizing nature of the $[Ag(succ)_4]^-$ ion, which is further manifested in the ability of $\mathbf{2}^{Cs}$ to oxidize water, forming succinimide, O_2, and a Ag^I complex $\mathbf{1}^{Cs}$. TDDFT computation of the lowest excitations in $\mathbf{2}^{Rb}$ reveal LMCT character (ligand-to-$Ag(d_{x^2-y^2})$) to dominate in the observed spectral range. Solid-state ^{109}Ag magic-angle spinning NMR studies reveal a resonance at 492 ppm for Ag^I precursor $\mathbf{1}^{Na}$, whereas Ag^{III} complex $\mathbf{2}^{Cs}$ exhibits a highly deshielded resonance at 2080 ppm, in the range expected for Ag^{III}, but towards the low end due to the covalent nature of the bonding in the trivalent silver complex with nitrogen donors. The NMR studies directly map the change in geometry between $\mathbf{1}^{Na}$ (linear) and $\mathbf{2}^{Cs}$ (square planar) through a change of sign for the shielding anisotropy (δ_σ). Moreover, the ^{109}Ag chemical shift of $\mathbf{2}^{Cs}$ is highly temperature-dependent (−32 ppm/°C), leading to variations of several hundred ppm within a temperature range of few °C. The possibility of generating $\mathbf{2}^{Cs}$ by chemical as well as electrochemical oxidation is of interest in both coordination chemistry and materials science, given that the identification of argentate(III) systems such as $[Ag(succ)_4]^-$ illustrates one possible fate of silver anodes used for electroplating. We are presently examining the new family of succinimide complexes as ditopic metalloligands and seeking entries to other Ag^{III} complexes to probe their reactivity and electronic structure.

Data availability

All experimental data are available in the ESI;† synthetic procedures; NMR, IR, UV-vis, X-ray diffraction, and magnetic data. CCDC entries 2365916–2365920, and 2372376 contain full crystallographic data (.cif) reported herein. The data supporting this article have been included as part of the ESI.†

Author contributions

The synthetic work was carried out by E. M. H. L., A. R. and J. B. All authors contributed to data collection and to writing the manuscript.

Conflicts of interest

There are no conflicts to declare.

Acknowledgements

JB acknowledges support from and the Independent Research Fund Denmark (1026-00082B).

Notes and references

1 (*a*) W. Levason and M. D. Spicer, *Coord. Chem. Rev.*, 1987, **76**, 45–120; (*b*) M. A. García-Monforte, S. Martínez-Salvador and B. Menjón, *Eur. J. Inorg. Chem.*, 2012, **2012**, 4945–4966.

2 (*a*) B. Zemva, K. Lutar, A. Jesih, W. J. Casteel, A. P. Wilkinson, D. E. Cox, R. B. Von Dreele, H. Borrmann and N. Bartlett, *J. Am. Chem. Soc.*, 1991, **113**, 4192–4198; (*b*) N. Bartlett, G. Lucier, C. Shen, W. J. Casteel, L. Chacon, J. Munzenberg and B. Žemva, *J. Fluorine Chem.*, 1995, **71**, 163–164; (*c*) J. Zhang, S. Huo, H. Shi, S. Shen and Y. Shang, *Transition Met. Chem.*, 2013, **38**, 15–20.

3 (*a*) J. A. Schlueter, K. D. Carlson, U. Geiser, H. H. Wang, J. M. Williams, W. K. Kwok, J. A. Fendrich, U. Welp, P. M. Keane, J. D. Dudek, A. S. Komosa, D. Naumann, T. Roy, J. E. Schirber, W. R. Bayless and B. Dodrill, *Phys. C: Supercond. Appl.*, 1994, **233**, 379–386; (*b*) J. A. Schlueter, L. Wiehl, H. Park, M. de Souza, M. Lang, H.-J. Koo and M.-H. Whangbo, *J. Am. Chem. Soc.*, 2010, **132**, 16308–16310; (*c*) D. Guterding, M. Altmeyer, H. O. Jeschke and R. Valentí, *Phys. Rev. B*, 2016, **94**, 024515.

4 U. Geiser, J. A. Schlueter, J. D. Dudek, J. M. Williams, D. Naumann and T. Roy, *Acta Crystallogr., Sect. C: Cryst. Struct. Commun.*, 1995, **51**, 1779–1782.

5 S. Weske, R. A. Hardin, T. Auth, R. A. J. O'Hair, K. Koszinowski and C. A. Ogle, *Chem. Commun.*, 2018, **54**, 5086–5089.

6 (*a*) M. Font, F. Acuña-Parés, T. Parella, J. Serra, J. M. Luis, J. Lloret-Fillol, M. Costas and X. Ribas, *Nat. Commun.*, 2014, **5**, 4373; (*b*) L. Capdevila, E. Andris, A. Briš, M. Tarrés, S. Roldán-Gómez, J. Roithová and X. Ribas, *ACS Catal.*, 2018, **8**, 10430–10436.

7 (*a*) L. Demonti, N. Saffon-Merceron, N. Mézailles and N. Nebra, *Chem.–Eur. J.*, 2021, **27**, 15396–15405; (*b*) Z. Lu, S. Liu, Y. Lan, X. Leng and Q. Shen, *Organometallics*, 2021, **40**, 1713–1718.

8 M. Deuker, Y. Yang, R. A. J. O'Hair and K. Koszinowski, *Organometallics*, 2021, **40**, 2354–2363.

9 (*a*) L. Malatesta, *Gazz. Chim. Ital.*, 1941, **71**, 467–474; (*b*) R. Masse and A. Simon, *J. Solid State Chem.*, 1982, **44**, 201–207; (*c*) C. J. Spina, J. E. Notarandrea-Alfonzo, E. D. Guerra, C. Goodall, D. S. Bohle and R. Precht, *ACS Omega*, 2021, **6**, 27017–27025; (*d*) L. Malaprade, *C. R. Acad. Sci.*, 1940, **210**, 504–505.

10 L. Malatesta, *Gazz. Chim. Ital.*, 1941, **71**, 580–584.

11 (*a*) P. Rây, *Nature*, 1943, **151**, 643; (*b*) P. Rây and K. Chakravarty, *J. Indian Chem. Soc.*, 1944, **21**, 47–50; (*c*) N. R. Kunchur, *Nature*, 1968, **217**, 539.

12 (*a*) L. F. Warren and M. A. Bennett, *Inorg. Chem.*, 1976, **15**, 3126–3140; (*b*) L. J. Kirschenbaum and J. D. Rush, *J. Am. Chem. Soc.*, 1984, **106**, 1003–1010; (*c*) L. J. Kirschenbaum, R. K. Panda, E. T. Borish and E. Mentasti, *Inorg. Chem.*, 1989, **28**, 3623–3628.

13 E. K. Barefield and M. T. Mocella, *Inorg. Chem.*, 1973, **12**, 2829–2832.

14 (*a*) H. Furuta, T. Ogawa, Y. Uwatoko and K. Araki, *Inorg. Chem.*, 1999, **38**, 2676–2682; (*b*) H. Furuta, H. Maeda and A. Osuka, *J. Am. Chem. Soc.*, 2000, **122**, 803–807; (*c*) M. A. Muckey, L. F. Szczepura, G. M. Ferrence and T. D. Lash, *Inorg. Chem.*, 2002, **41**, 4840–4842; (*d*) C. Brückner, C. A. Barta, R. P. Briñas and J. A. Krause Bauer, *Inorg. Chem.*, 2003, **42**, 1673–1680; (*e*) H. Furuta, T. Morimoto and A. Osuka, *Org. Lett.*, 2003, **5**, 1427–1430; (*f*) H. Maeda, A. Osuka, Y. Ishikawa, I. Aritome, Y. Hisaeda and H. Furuta, *Org. Lett.*, 2003, **5**, 1293–1296; (*g*) M. Pawlicki and L. Latos-Grażyński, *Chem.–Eur. J.*, 2003, **9**, 4650–4660; (*h*) K. M. Bergman, G. M. Ferrence and T. D. Lash, *J. Org. Chem.*, 2004, **69**, 7888–7897; (*i*) M. Pawlicki and L. Latos-Grażyński, *J. Org. Chem.*, 2005, **70**, 9123–9130; (*j*) M. Stefanelli, M. Mastroianni, S. Nardis, S. Licoccia, F. R. Fronczek, K. M. Smith, W. Zhu, Z. Ou, K. M. Kadish and R. Paolesse, *Inorg. Chem.*, 2007, **46**, 10791–10799; (*k*) K. E. Thomas, A. B. Alemayehu, J. Conradie, C. Beavers and A. Ghosh, *Inorg. Chem.*, 2011, **50**, 12844–12851; (*l*) W. Sinha, M. G. Sommer, N. Deibel, F. Ehret, B. Sarkar and S. Kar, *Chem.–Eur. J.*, 2014, **20**, 15920–15932; (*m*) K. E. Thomas, H. Vazquez-Lima, Y. Fang, Y. Song, K. J. Gagnon, C. M. Beavers, K. M. Kadish and A. Ghosh, *Chem.–Eur. J.*, 2015, **21**, 16839–16847; (*n*) M. Soll, K. Sudhakar, N. Fridman, A. Müller, B. Röder and Z. Gross, *Org. Lett.*, 2016, **18**, 5840–5843; (*o*) J. Yan, Y. Yang, M. Ishida, S. Mori, B. Zhang, Y. Feng and H. Furuta, *Chem.–Eur. J.*, 2017, **23**, 11375–11384; (*p*) C. M. Lemon, D. C. Powers, M. Huynh, A. G. Maher, A. A. Phillips, B. P. Tripet and D. G. Nocera, *Inorg. Chem.*, 2023, **62**, 3–17.

15 R. Hoppe, *Z. Anorg. Allg. Chem.*, 1957, **292**, 28–33.

16 R. Hoppe and R. Homann, *Naturwissenschaften*, 1966, **53**, 501.

17 G. L. Cohen and G. Atkinson, *J. Electrochem. Soc.*, 1968, **115**, 1236–1242.

18 (*a*) G. L. Cohen and G. Atkinson, *Inorg. Chem.*, 1964, **3**, 1741–1743; (*b*) L. J. Kirschenbaum, J. H. Ambrus and G. Atkinson, *Inorg. Chem.*, 1973, **12**, 2832–2837.

19 J. Iqbal, D. W. A. Sharp and J. M. Winfield, *J. Chem. Soc., Dalton Trans.*, 1989, 461–464.

20 (*a*) W. Dukat and D. Naumann, *Rev. Chim. Miner.*, 1986, **23**, 589–603; (*b*) L. Demonti, H. Tabikh, N. Saffon-Merceron and N. Nebra, *Eur. J. Inorg. Chem.*, 2023, **26**, e202300042.

21 (*a*) R. Eujen, B. Hoge and D. J. Brauer, *Inorg. Chem.*, 1997, **36**, 3160–3166; (*b*) D. Joven-Sancho, M. Baya, A. Martín and B. Menjón, *Chem.–Eur. J.*, 2018, **24**, 13098–13101; (*c*) M. Baya, D. Joven-Sancho, P. J. Alonso, J. Orduna and B. Menjón, *Angew. Chem., Int. Ed.*, 2019, **58**, 9954–9958.

22 (*a*) R. Eujen, B. Hoge and D. J. Brauer, *Inorg. Chem.*, 1997, **36**, 1464–1475; (*b*) D. Joven-Sancho, M. Baya, L. R. Falvello, A. Martín, J. Orduna and B. Menjón, *Chem.–Eur. J.*, 2021, **27**, 12796–12806; (*c*) D. Joven-Sancho, M. Baya, A. Martín, J. Orduna and B. Menjón, *Chem.–Eur. J.*, 2020, **26**, 4471–4475.

23 (*a*) D. Naumann, W. Tyrra, F. Trinius, W. Wessel and T. Roy, *J. Fluorine Chem.*, 2000, **101**, 131–135; (*b*) D. Joven-Sancho, L. Demonti, A. Martín, N. Saffon-Merceron, N. Nebra, M. Baya and B. Menjón, *Chem. Commun.*, 2023, **59**, 4166–4168; (*c*) J. Pueyo, D. Joven-Sancho, A. Martín, B. Menjón and M. Baya, *Chem.–Eur. J.*, 2024, **30**, e202303937; (*d*) L. Demonti, D. Joven-Sancho, N. Saffon-Merceron, M. Baya and N. Nebra, *Chem.–Eur. J.*, 2024, **30**, e202400881.

24 D. Joven-Sancho, M. Baya, A. Martín, J. Orduna and B. Menjón, *Angew. Chem., Int. Ed.*, 2021, **60**, 26545–26549.

25 (*a*) D. Naumann, T. Roy, K.-F. Tebbe and W. Crump, *Angew. Chem., Int. Ed. Engl.*, 1993, **32**, 1482–1483; (*b*) N. Nebra and V. V. Grushin, *J. Am. Chem. Soc.*, 2014, **136**, 16998–17001; (*c*) A. M. Romine, N. Nebra, A. I. Konovalov, E. Martin, J. Benet-Buchholz and V. V. Grushin, *Angew. Chem., Int. Ed.*, 2015, **54**, 2745–2749.
26 M. Kaupp and H. G. von Schnering, *Angew. Chem., Int. Ed. Engl.*, 1995, **34**, 986.
27 R. Hoffmann, S. Alvarez, C. Mealli, A. Falceto, T. J. Cahill, T. Zeng and G. Manca, *Chem. Rev.*, 2016, **116**, 8173–8192.
28 J. P. Snyder, *Angew. Chem., Int. Ed. Engl.*, 1995, **34**, 80–81.
29 (*a*) R. C. Walroth, J. T. Lukens, S. N. MacMillan, K. D. Finkelstein and K. M. Lancaster, *J. Am. Chem. Soc.*, 2016, **138**, 1922–1931; (*b*) I. M. DiMucci, J. T. Lukens, S. Chatterjee, K. M. Carsch, C. J. Titus, S. J. Lee, D. Nordlund, T. A. Betley, S. N. MacMillan and K. M. Lancaster, *J. Am. Chem. Soc.*, 2019, **141**, 18508–18520.
30 C. Gao, G. Macetti and J. Overgaard, *Inorg. Chem.*, 2019, **58**, 2133–2139.
31 J. P. Snyder, *Angew. Chem., Int. Ed. Engl.*, 1995, **34**, 986–987.
32 (*a*) W. Grochala and R. Hoffmann, *Angew. Chem., Int. Ed.*, 2001, **40**, 2742–2781; (*b*) W. Grochala, R. G. Egdell, P. P. Edwards, Z. Mazej and B. Žemva, *ChemPhysChem*, 2003, **4**, 997–1001; (*c*) W. Grochala and Z. Mazej, *Philos. Trans. R. Soc., A*, 2015, **373**, 20140179.
33 R. J. Deeth, *Phys. Chem. Chem. Phys.*, 2024, **26**, 18138–18148.
34 (*a*) T. J. Collins, *Acc. Chem. Res.*, 1994, **27**, 279–285; (*b*) T. J. Collins, T. R. Nichols and E. S. Uffelman, *J. Am. Chem. Soc.*, 1991, **113**, 4708–4709; (*c*) F. T. de Oliveira, A. Chanda, D. Banerjee, X. Shan, S. Mondal, L. Que, E. L. Bominaar, E. Münck and T. J. Collins, *Science*, 2007, **315**, 835–838; (*d*) M. R. Mills, A. C. Weitz, M. P. Hendrich, A. D. Ryabov and T. J. Collins, *J. Am. Chem. Soc.*, 2016, **138**, 13866–13869; (*e*) F. C. Anson, T. J. Collins, T. G. Richmond, B. D. Santarsiero, J. E. Toth and B. G. R. T. Treco, *J. Am. Chem. Soc.*, 1987, **109**, 2974–2979.
35 (*a*) S. Jayakrishnan, S. R. Natarajan and K. I. Vasu, *Met. Finish.*, 1996, **94**, 12–15; (*b*) S. Masaki, H. Inoue and K. Yamakawa, *J. Surf. Finish. Soc. Jpn.*, 1997, **48**, 559–564; (*c*) S. Masaki, H. Inoue and K. Yamakawa, *J. Surf. Finish. Soc. Jpn.*, 1997, **48**, 643–646.
36 J.-Y. Huot, D. Serve and J. Lessard, *Can. J. Chem.*, 1983, **61**, 1890–1898.
37 J.-Y. Huot, D. Serve, S. Desjardins and J. Lessard, *Can. J. Chem.*, 1988, **66**, 35–44.
38 S. Masaki, H. Inoue and H. Honma, *Met. Finish.*, 1998, **96**, 52–54.
39 (*a*) G. A. Barbieri, *Gazz. Chim. Ital.*, 1912, **42**, 7–14; (*b*) G. B. Kauffman, R. A. Houghten, R. E. Likins, P. L. Posson, R. K. Ray, J. P. Fackler Jr and R. Theron Stubbs, *Inorg. Synth.*, 1998, 177–181.
40 (*a*) W. Khayata, D. Baylocq, F. Pellerin and N. Rodier, *Acta Crystallogr., Sect. C: Cryst. Struct. Commun.*, 1984, **40**, 765–767; (*b*) J. Perron and A. L. Beauchamp, *Inorg. Chem.*, 1984, **23**, 2853–2859; (*c*) X. Tao, K.-C. Shen, Y.-L. Wang and Y.-Z. Shen, *Z. Anorg. Allg. Chem.*, 2011, **637**, 1394–1400.
41 (*a*) E. I. Solomon, P. Chen, M. Metz, S.-K. Lee and A. E. Palmer, *Angew. Chem., Int. Ed.*, 2001, **40**, 4570–4590; (*b*) M. Atanasov, C. A. Daul and C. Rauzy, *Chem. Phys. Lett.*, 2003, **367**, 737–746.
42 A. W. Addison, T. N. Rao, J. Reedijk, J. van Rijn and G. C. Verschoor, *J. Chem. Soc., Dalton Trans.*, 1984, 1349–1356.
43 M. B. Robin and P. Day, in *Advances in Inorganic Chemistry and Radiochemistry*, ed. H. J. Emeléus and A. G. Sharpe, Academic Press, 1968, vol. 10, pp. 247–422.
44 T. Woldbæk, P. Klæboe and D. H. Christensen, *Acta Chem. Scand.*, 1976, **30A**, 531–539.
45 (*a*) L. H. Merwin and A. Sebald, *J. Magn. Reson.*, 1992, **97**, 628–631; (*b*) L. van Wüllen, S. Vensky, W. Hoffbauer and M. Jansen, *Solid State Sci.*, 2005, **7**, 920–924; (*c*) G. H. Penner and X. Liu, *Prog. Nucl. Magn. Reson. Spectrosc.*, 2006, **49**, 151–167; (*d*) G. H. Penner and W. Li, *Inorg. Chem.*, 2004, **43**, 5588–5597.
46 R. Eujen and B. Zemva, *J. Fluorine Chem.*, 1999, **99**, 139–140.
47 (*a*) P. J. Leszczynski, M. J. Jadwiszczak and W. Grochala, *ChemistrySelect*, 2023, **8**, e202301775; (*b*) L. Demonti, D. Joven-Sancho and N. Nebra, *Chem. Rec.*, 2023, **23**, e202300143.
48 M. Weil, M. Puchberger, E. Füglein, E. J. Baran, J. Vannahme, H. J. Jakobsen and J. Skibsted, *Inorg. Chem.*, 2007, **46**, 801–808.
49 G. A. Bowmaker, R. K. Harris, B. Assadollahzadeh, D. C. Apperley, P. Hodgkinson and P. Amornsakchai, *Magn. Reson. Chem.*, 2004, **42**, 819–826.
50 Ö. Üngör, T. M. Ozvat, Z. Ni and J. M. Zadrozny, *J. Am. Chem. Soc.*, 2022, **144**, 9132–9137.